

RESEARCH ARTICLE

MEDICINE

Mitochondrial remodeling and ischemic protection by G protein-coupled receptor 35 agonists

Gregory A. Wyant^{1,2}, Wenyu Yu¹, Ilias P. Doulamis³, Rio S. Nomoto³, Mossab Y. Saeed³, Thomas Duignan³, James D McCullly³, William G. Kaelin, Jr.^{1,2,4*}

Kynurenic acid (KynA) is tissue protective in cardiac, cerebral, renal, and retinal ischemia models, but the mechanism is unknown. KynA can bind to multiple receptors, including the aryl hydrocarbon receptor, the $\alpha 7$ nicotinic acetylcholine receptor ($\alpha 7$ nAChR), multiple ionotropic glutamate receptors, and the orphan G protein-coupled receptor GPR35. Here, we show that GPR35 activation was necessary and sufficient for ischemic protection by KynA. When bound by KynA, GPR35 activated G_i and $G_{12/13}$ -coupled signaling and trafficked to the outer mitochondrial membrane, where it bound, apparently indirectly, to ATP synthase inhibitory factor subunit 1 (ATPIF1). Activated GPR35, in an ATPIF1-dependent and pertussis toxin-sensitive manner, induced ATP synthase dimerization, which prevented ATP loss upon ischemia. These findings provide a rationale for the development of specific GPR35 agonists for the treatment of ischemic diseases.

Kynurenic acid (KynA) has been shown to protect tissues in preclinical organ ischemia models and to mediate cardioprotection in a mouse model of remote ischemic preconditioning, a phenomenon whereby an ischemic tissue confers ischemic protection to other tissues at a distance (1–5). Mice, however, are a suboptimal model for cardiac physiology studies because of their small size, extremely rapid heart rates, and short life spans (6). Therefore, we tested KynA in rabbits. Pretreatment of rabbits with KynA decreased infarct size when their excised, beating, and perfused hearts (Langendorff prep) were subjected to a brief period of ischemia followed by reperfusion to model ischemia/reperfusion (I/R) injury (fig. S1, A to D). KynA also increased cardiac function after I/R, as measured by increased fractional shortening, increased left ventricular contractility (dP/dt max), and left ventricular peak developed pressure (LVPDP) during reperfusion (fig. S1, E to H).

We tested which of the putative KynA receptors (7–13), if any, mediated KynA's tissue-protective effects. Because KynA protects isolated hearts against ischemia, we focused on the aryl hydrocarbon receptor (AhR) and G protein-coupled receptor 35 (GPR35) rather than on ionotropic glutamate receptors, which are linked to neurotransmission. KynA promoted the binding of the AhR to its partner,

aryl hydrocarbon receptor nuclear translocator (ARNT), and activated AhR-responsive transcription (fig. S2, A and B). However, cardiac AhR loss in mice did not block KynA-induced cardioprotection in the setting of I/R injury *in vivo* (fig. S2, C and D). Moreover, stable expression of a constitutively active *AHR* (*AHR-CA*) cardiomyocytes derived from human induced pluripotent stem (hIPS) cells did not promote their survival when they were transiently deprived of oxygen and nutrients and then re-exposed to oxygen and nutrients to simulate I/R injury *ex vivo* (fig. S2, E to G). Therefore, AhR activation is neither necessary nor sufficient for KynA-induced cardioprotection.

GPR35 is broadly expressed, and its abundance is increased after hypoxia under the control of the HIF α transcription factor and also in human heart failure (fig. S3, A to C) (14, 15). Moreover, GPR35 is linked to tissue protection, although studies disagree as to whether GPR35 agonism or antagonism is protective (16–18). Whether KynA is an authentic endogenous GPR35 ligand is also controversial, partly because its binding affinity for GPR35 varies across species and, in some species, is relatively low (in the micromolar range) (19).

We confirmed that radiolabeled KynA bound to purified human and mouse GPR35 (Fig. 1A). This was specific, because radiolabeled KynA did not bind to a control G protein-coupled receptor (GPCR), GPR160, and its binding to GPR35 was prevented by excess unlabeled KynA and the known GPR35 activators pamoic acid, zaprinast, and lodoxamide, but not by the KynA-derived metabolite quinolinic acid or tryptophan (the parent molecule from which KynA is derived) (Fig. 1B) (20–22). KynA activated G_i and $G_{12/13}$ in a GPR35-dependent manner,

as determined by G_i and $G_{12/13}$ recruitment, activation of the protein kinase Rho, and suppression of forskolin-induced cAMP abundance and downstream signaling by protein kinase A (PKA) (fig. S4, A to E).

We sought to create a GPR35 mutant that could not bind to KynA so that it could be used as a specificity control. We made a series of GPR35 missense mutants in which specific residues within GPR35 transmembrane domains III and IV were converted to alanine, motivated by previous homology modeling and ligand-docking studies that implicated this region (particularly specific arginine residues within this region) in ligand binding (23, 24). One such variant, GPR35 R151A, failed to bind to radiolabeled KynA in assays using GPR35-expressing cell membrane fractions or highly purified GPR35 (Fig. 1, C to F). Similarly, KynA bound to wild-type GPR35, but not GPR35 R151A, in thermal shift assays based on thermostabilization upon ligand binding (Fig. 1G). Because these studies used GPR35 that was purified from mammalian cells (293T cells), we cannot yet formally exclude that additional cellular proteins are required for the binding of KynA to GPR35. Many GPCRs, including GPR35, are internalized upon activation (25). We confirmed that wild-type GPR35, but not GPR35 R151A, was internalized in early endosome antigen 1 (EEA1)-containing endosomes in cells treated with KynA or the GPR35 agonists pamoic acid or zaprinast, but not in cells treated with quinolinic acid (Fig. 1H and fig. S5A) (11, 15). GPR35-containing endosomes also contained transferrin receptor (TFR), which is normally present on plasma membranes, consistent with the GPR35 endosomes participating in endosomal trafficking (fig. S5B). β -arrestin localization was not regulated by KynA or by the GPR35 agonist pamoic acid in the cardiomyocytes that we studied, although it is regulated by many other GPCRs that are internalized upon activation (fig. S5C) (25).

Cardioprotection by KynA administered either 2 or 24 hours before injury *in vivo* or 10 or 30 min before I/R in *ex vivo* hearts was completely abrogated in GPR35^{−/−} mice that we made using CRISPR/Cas9-based gene editing of mouse embryos (Fig. 2, A and B, and fig. S6A) (26). GPR35 loss did not alter, either positively or negatively, the induction of hypoxia-inducible transcription factor 1 α (HIF1 α) after cardiac I/R injury (fig. S6B). In cell culture experiments performed with murine neonatal cardiomyocytes, KynA, in a GPR35-dependent manner, decreased resting oxygen consumption and, after simulated I/R injury, decreased mitochondrial reactive oxygen species production and preserved mitochondrial membrane potential (fig. S6, C to E), changes that would be predicted to promote survival after I/R.

The drug FG-4592 (roxadustat), which stabilizes HIF1 α by inactivating the egg laying

¹Department of Medical Oncology, Dana-Farber Cancer Institute, Boston, MA 02215, USA. ²Howard Hughes Medical Institute, Chevy Chase, MD 20815, USA. ³Department of Cardiac Surgery, Boston Children's Hospital, Department of Surgery, Harvard Medical School, Boston, MA 02115, USA. ⁴Department of Medicine, Brigham and Women's Hospital, Harvard Medical School, Boston, MA 02215, USA.

*Corresponding author. Email: william_kaelin@dfci.harvard.edu

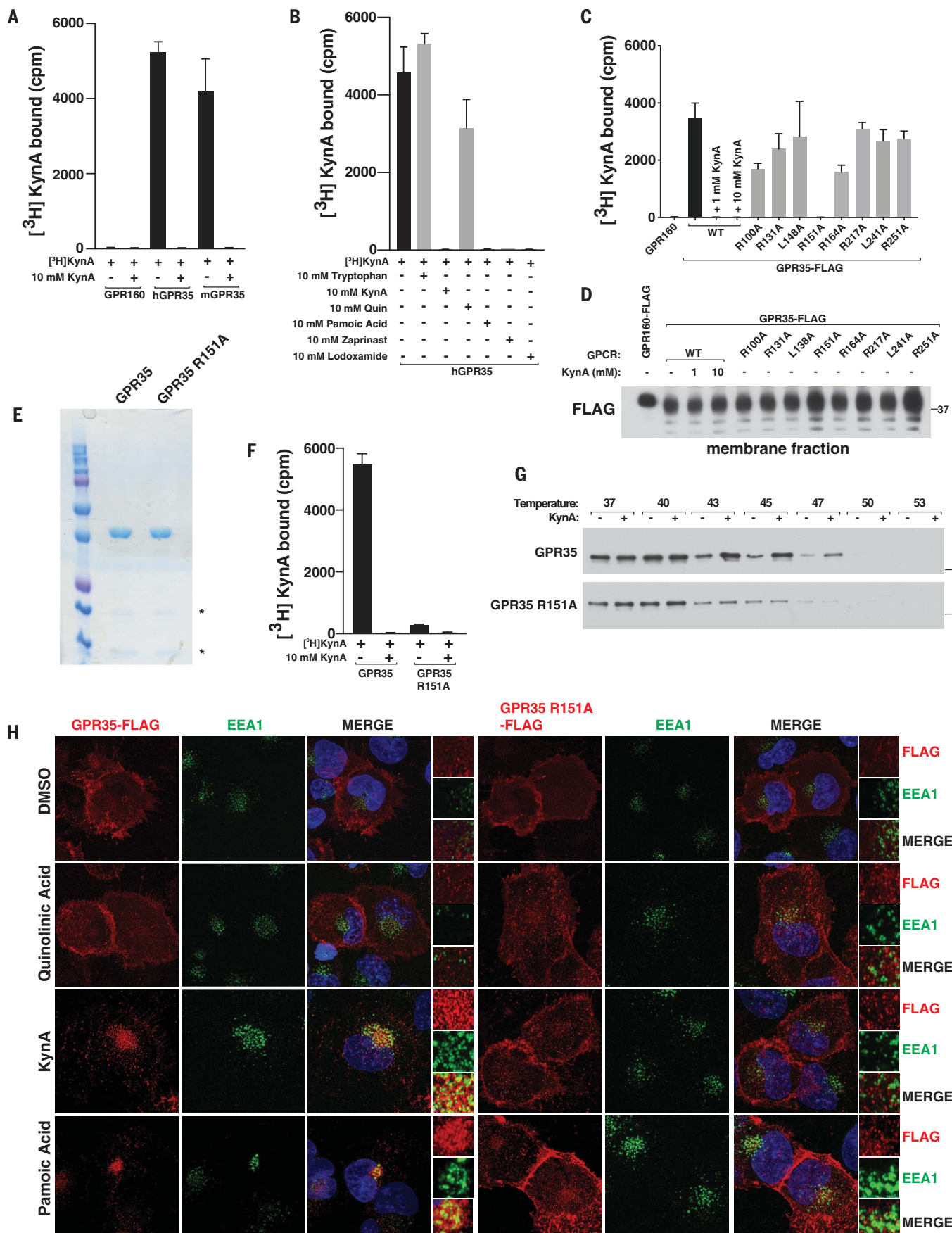


Fig. 1. KynA binds GPR35 and promotes GPR35 internalization. (A, B, and F) [³H]-KynA-binding assay using tandem affinity-purified versions of the indicated high-density lipoprotein-reconstituted hemagglutinin (HA)-FLAG-tagged GPCRs in the presence or absence of the indicated unlabeled competitor compounds (10 mM). (C and D) [³H]-KynA binding (C) and immunoblot (D) assays of isolated membrane fractions from 293T cells expressing FLAG-GPR160 or FLAG-GPR35 (wild-type or mutant). Where indicated, 1 and 10 mM unlabeled KynA was used as a competitor. (E and G) Commissie

blue staining (E) and immunoblot (G) assay of the purified GPCRs used in (F). In (G), the proteins were preincubated with 1 mM KynA or dimethyl sulfoxide (DMSO) for 1 hour before exposure to the indicated temperatures. (H) Confocal microscopy of mouse neonatal cardiomyocytes stably expressing wild-type or R151A GPR35-FLAG stimulated with 20 μ M quinolinic acid, 20 μ M KynA, or 1 μ M pamoic acid for 20 min. Scale bar, 20 μ m. In (A), (B), (C), and (F), values are shown as means \pm SDs for three technical replicates from one representative experiment.

defective 9 (EGLN) prolyl hydroxylases, was shown to be cardioprotective in preclinical models (27–29). Cardioprotection is likely an on-target effect of FG-4592 because similar effects have been observed with other structurally unrelated EGLN inhibitors and after systemic or cardiac-specific genetic inactivation of EGLN1, which is the primary regulator of HIF1 α stability (1, 28, 30–32). Although EGLN inactivation is thought to cardioprotect by stabilizing HIF1 α , systemic inactivation of EGLN also increases the plasma concentrations of 2-oxoglutarate (2-OG), which is converted to KynA by the liver and released into the circulation (1). Cardiac protection by FG-4592 in vivo was partially abrogated by loss of GPR35 (Fig. 2A). By contrast, FG-4592 was cardioprotective in wild-type and GPR35 $^{-/-}$ hearts when administered ex vivo, a setting in which KynA would not be produced, before I/R (Fig. 2, B and C). Protection by FG-4592 was observed when given 30 min, but not 10 min, before I/R, which correlated with successful induction of HIF1 α 30 min after FG-4592 administration (Fig. 2C). By contrast, KynA protected more rapidly (Fig. 2B). These results suggest that cardiac protection in vivo by roxadustat is caused by the direct effects of HIF1 α and the indirect effects on GPR35 mediated by endogenous KynA.

Pertussis toxin, a classic G_i and G_o protein family inhibitor, abolished cardiac ischemic preconditioning in rats (33) and likewise inhibited KynA-induced cardiac ischemic protection in vivo, suggesting that intact G_i or G_o family signaling by GPR35 is required for KynA-induced ischemic protection (Fig. 2D). Multiple structurally unrelated GPR35 agonists, including Iodoamphetamine, zaprinast, and pamoic acid, were cardioprotective in vivo and ex vivo, whereas quinolinic acid, which fails to activate GPR35, was not (Fig. 2, E and F). Where tested, cardioprotection by these other GPR35 agonists was GPR35 dependent (Fig. 2A).

To formally test whether KynA binding to GPR35 is necessary for KynA-induced ischemic protection, we used CRISPR-Cas9 to generate HIPS cells lacking GPR35 and then infected them with a lentivirus encoding wild-type GPR35, GPR35 R151A, or the empty vector (Fig. 2G). These cells were then induced to become cardiomyocytes and subjected to simulated I/R ex vivo. KynA pretreatment protected against I/R-induced injury, and this

protection was lost in the absence of GPR35. Reexpression of the wild-type GPR35, but not GPR35 R151A, in the GPR35 $^{-/-}$ cardiomyocytes restored protection by KynA (Fig. 2H). Thus, GPR35 mediates KynA-induced ischemic protection in both mouse and human cells, and this protection requires the binding of KynA to GPR35.

GPR35 is annotated to bind to the mitochondrial protein ATP synthase inhibitory factor subunit 1 (ATPIF1) and ATP synthase in the BioPlex protein-protein interaction database (34). To test whether GPR35 can associate with mitochondria, we reintroduced wild-type or R151A GPR35 into GPR35 $^{-/-}$ murine neonatal cardiomyocytes by lentiviral infection. Treatment of the wild-type cells with GPR35 agonists, including KynA, led to colocalization of GPR35 with mitochondrial proteins such as citrate synthase and the ATP synthase component ATP5H, but not the Golgi apparatus protein GM130 or the endoplasmic reticulum protein calreticulin, as shown by confocal microscopy and quantitative image analysis (Fig. 3A and figs. S7, A to C, and S8, A to D). This was specific because colocalization with mitochondria was not observed with GPR35 R151A or with quinolinic acid. KynA and the GPR35 agonist pamoic acid, but not quinolinic acid, also increased GPR35 and TOM20 association in situ based on proximity ligation assays (fig. S7, D to E). To visualize GPR35 trafficking to mitochondria, we transiently overexpressed GPR35-GFP together with mCherry-TOMM20 in GPR35 $^{-/-}$ murine cardiomyocytes and performed live-cell imaging. KynA treatment caused GPR35-GFP to become internalized within minutes on cytoplasmic punctae that associated with mCherry-TOMM20 (fig. S8E). To corroborate these findings, we rapidly isolated mitochondria from cells expressing 3XHA-EGFP-OMP25 (HA-MITO) after KynA treatment and then performed immunoblot assays (35). We reproducibly detected the association of GPR35 with mitochondria, and this was increased in cells treated with KynA or other GPR35 agonists, but not in cells treated with quinolinic acid (Fig. 3B and fig. S9A). We introduced a biotin ligase (APEX) fused to wild-type or R151A GPR35 into the GPR35 $^{-/-}$ murine cardiomyocytes and captured GPR35-associated proteins using streptavidin agarose after treatment with biotin tyramide and hydrogen peroxide (to activate the APEX enzyme) in the presence

or absence of GPR35 agonists (fig. S9B) (36). Multiple mitochondrial outer membrane proteins, such as VDAC, TOM20, and TOM70, were associated with wild-type, but not R151A, GPR35 in cells treated with KynA (Fig. 3C). Similarly, KynA promoted biotin labeling of mitochondria, as determined by confocal microscopy using streptavidin-568 as a probe, in cells expressing wild-type GPR35-APEX, but not in those expressing GPR35 R151A-APEX (fig. S9C) (37).

We confirmed, using two different epitope tags, that epitope-tagged human and mouse GPR35 coimmunoprecipitated with endogenous ATPIF1 and ATP synthase, as determined by immunoblot analysis (fig. S10, A to D). Consistent with our localization studies, the binding of GPR35 to ATPIF1 was enhanced by KynA and the GPR35 agonists zaprinast and pamoic acid, but not by quinolinic acid (Fig. 4A and fig. S10A). As additional specificity controls, we looked for binding of ATPIF1 to cytosolic METAP2, the transmembrane mitochondrial protein TMEM141, GPR160, or a GPR35 C-terminal truncation mutant (Fig. 4B and fig. S10B), but found none. The electrophoretic mobility of wild-type GPR35 was decreased under these gel conditions compared with the C-terminal truncation mutant because of a slightly higher molecular size and because of glycosylation events that require the GPR35 C terminus (38).

ATPIF1 binds to, and regulates, the multimeric ATP synthase complex (39). The ATP synthase subunits ATP5B, ATP5H, ATP5O, and ATP5F1 also coimmunoprecipitated with GPR35, and their abundance mirrored that of ATPIF1 (Fig. 4, A and B, and fig. S10, A to C). Given that ATPIF1 and ATP synthase are localized inside mitochondria, we tested whether GPR35 is present inside or outside mitochondria after treatment with KynA. We treated murine cardiomyocytes expressing wild-type GPR35 with KynA and used differential centrifugation to purify mitochondria, which were then exposed to increasing amounts of proteinase K. Mitochondrially associated GPR35 was proteinase K sensitive, arguing that it is largely associated with the outer mitochondrial membrane (Fig. 4C). Consistent with this, KynA promoted GPR35-APEX biotinylation of the outer mitochondrial membrane proteins VDAC and TOM70, but did not promote biotinylation of ATPIF1 or ATP synthase

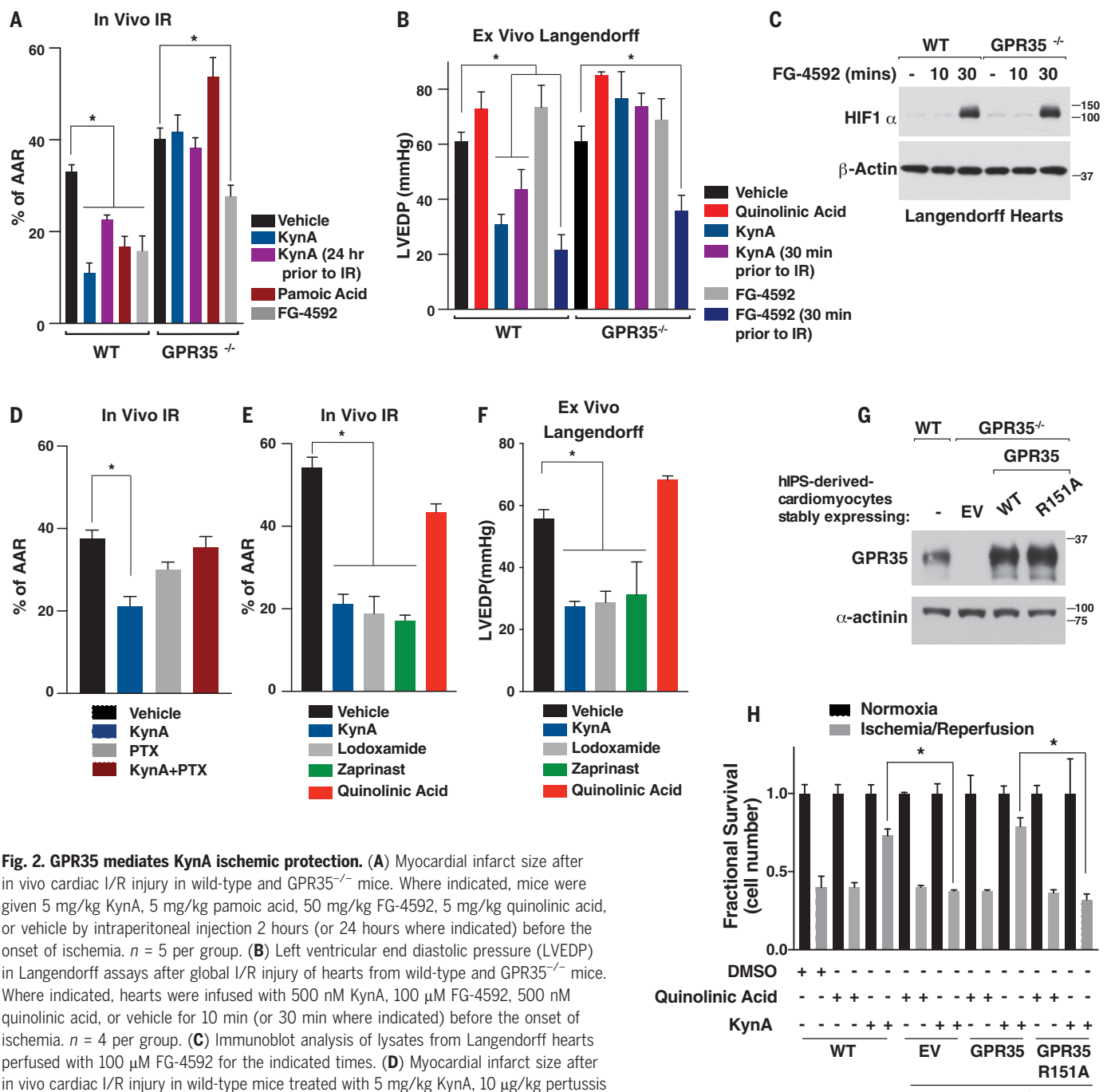


Fig. 2. GPR35 mediates KynA ischemic protection. (A) Myocardial infarct size after in vivo cardiac I/R injury in wild-type and GPR35^{-/-} mice. Where indicated, mice were given 5 mg/kg KynA, 5 mg/kg pamoic acid, 50 mg/kg FG-4592, 5 mg/kg quinolinic acid, or vehicle by intraperitoneal injection 2 hours (or 24 hours where indicated) before the onset of ischemia. $n = 5$ per group. (B) Left ventricular end diastolic pressure (LVEDP) in Langendorff assays after global I/R injury of hearts from wild-type and GPR35^{-/-} mice. Where indicated, hearts were infused with 500 nM KynA, 100 μ M FG-4592, 500 nM quinolinic acid, or vehicle for 10 min (or 30 min where indicated) before the onset of ischemia. $n = 4$ per group. (C) Immunoblot analysis of lysates from Langendorff hearts perfused with 100 μ M FG-4592 for the indicated times. (D) Myocardial infarct size after in vivo cardiac I/R injury in wild-type mice treated with 5 mg/kg KynA, 10 μ g/kg pertussis toxin (PTX), both, or vehicle by intraperitoneal injection. Mice were treated with KynA or vehicle 2 hours before or with PTX 24 hours before the onset of ischemia. $n = 4$ per group.

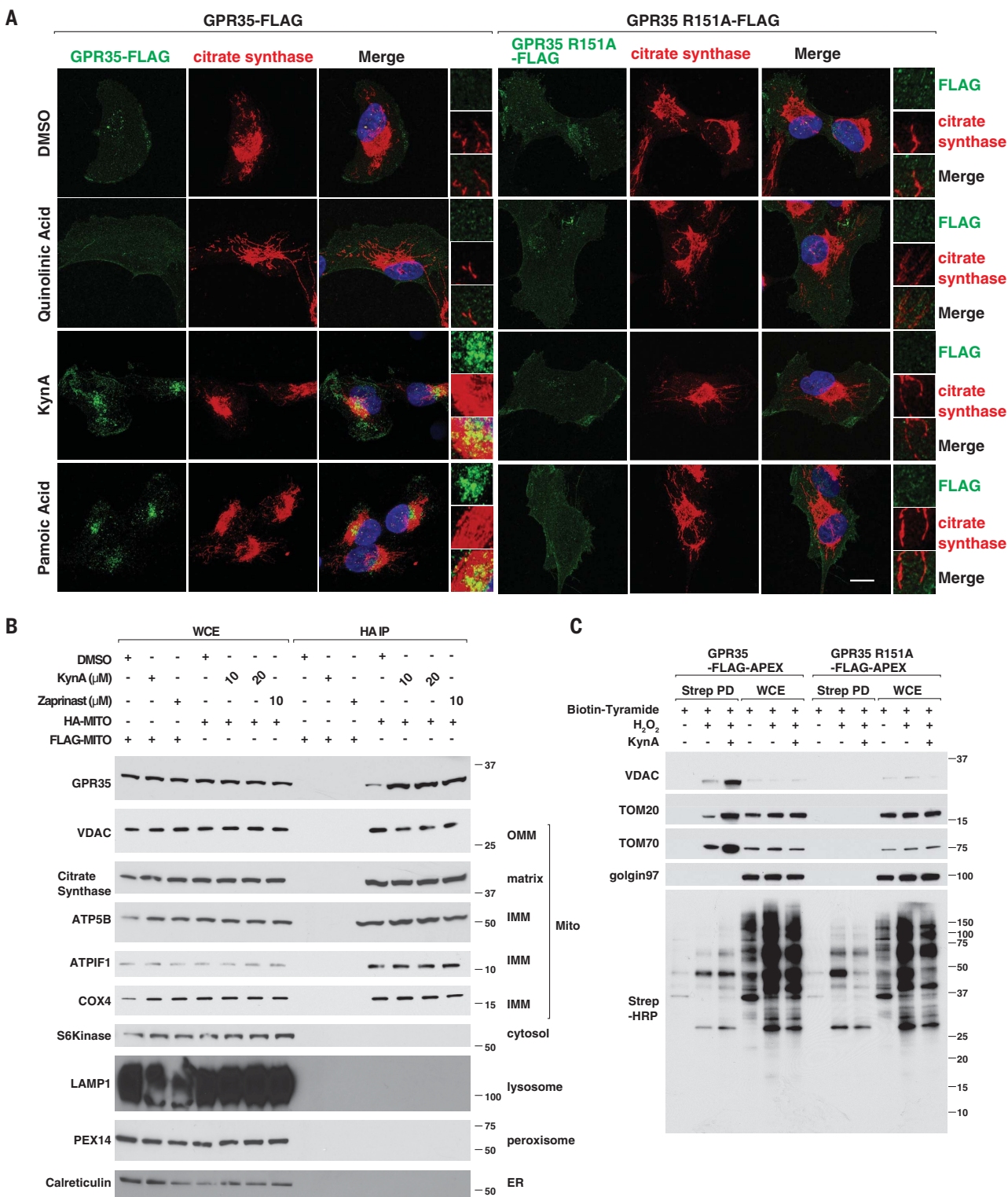
(E) Myocardial infarct size after in vivo cardiac I/R injury in wild-type mice given GPR35 agonists. Where indicated, mice were given 5 mg/kg KynA, 5 mg/kg lodoxamide, 5 mg/kg zaprinast, 5 mg/kg quinolinic acid, or vehicle by intraperitoneal injection 2 hours before the onset of ischemia. $n = 4$ per group. (F) LVEDP in Langendorff assays after global I/R injury. Where indicated, hearts were infused with 500 nM KynA, 1 μ M lodoxamide, 1 μ M zaprinast, 500 nM quinolinic acid, or vehicle for 10 min before the onset of ischemia. $n = 4$ per group. (G) Immunoblot of wild-type or GPR35^{-/-} hIPS-derived cardiomyocytes stably expressing wild-type or R151A GPR35. (H) Fractional survival after simulated I/R injury ex vivo of hIPS cell-derived cardiomyocytes modified as in (G). Cells were pretreated with 20 μ M KynA, 20 μ M quinolinic acid, or DMSO for 1 hour before I/R. Data are shown as mean \pm SD. * $P < 0.05$.

(Fig. 4D). Therefore, KynA promotes the association of GPR35 with ATPIF1 and ATP synthase, but this interaction is likely indirect.

During ischemia, ATP synthase shifts from ATP synthesis to ATP hydrolysis, with loss of ATP eventually contributing to cell death (40).

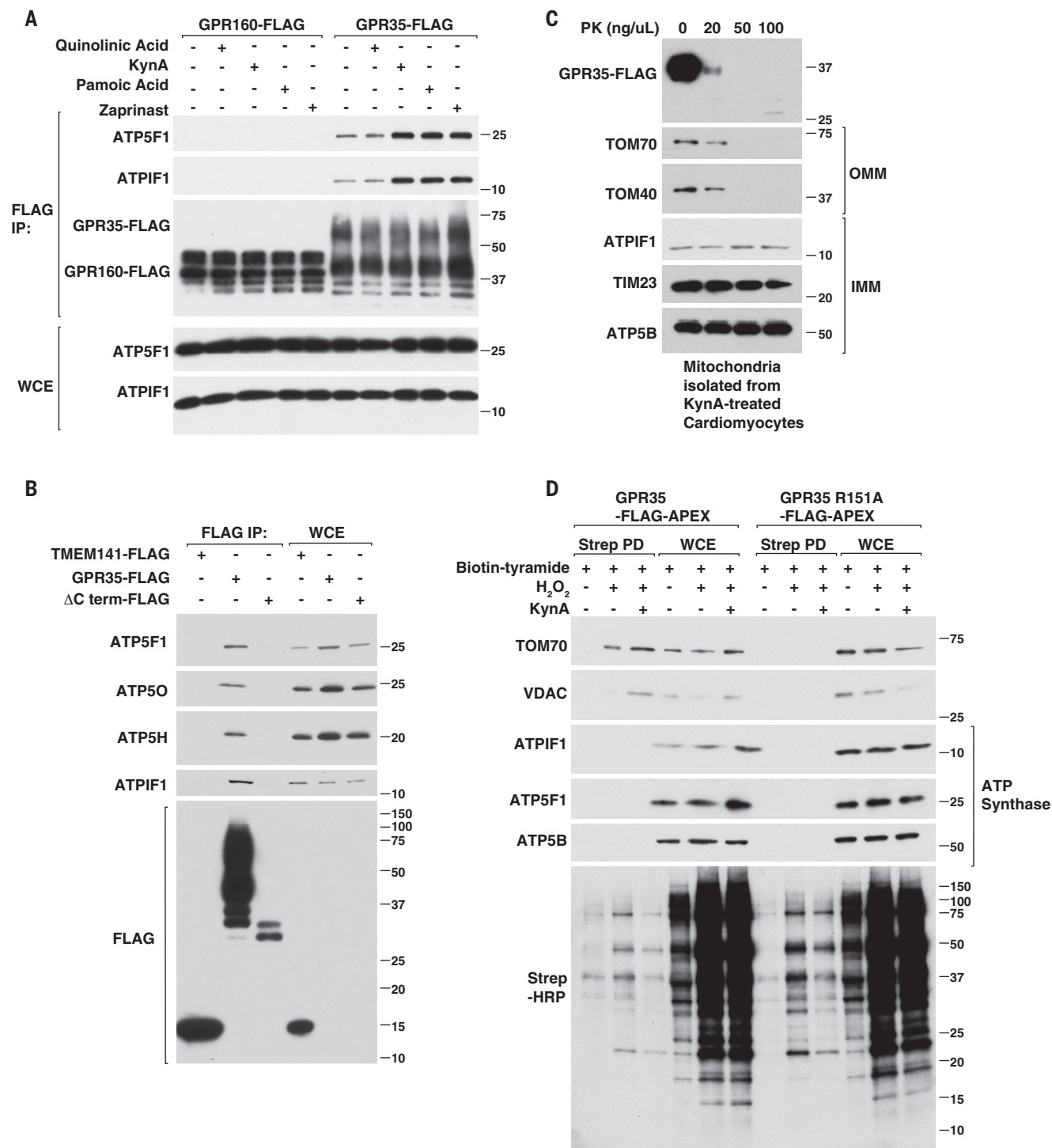
Binding of ATPIF1 to ATP synthase promotes the formation of ATP synthase dimers and thereby inhibits ATP hydrolysis, oxidative phosphorylation, and oxygen consumption (41–44). ATPIF1 mimetic compounds and transgenic overexpression of ATPIF1 both

protect tissues in I/R models (44, 45). Here, KynA increased the recovery of ATP synthase after immunoprecipitation of ATPIF1 and decreased the recovery of ATPIF1 after the immunoprecipitation of ATP synthase in a pertussis toxin-sensitive manner, consistent



Downloaded from https://www.science.org at University Van Amsterdam on April 13, 2025

Fig. 3. KynA promotes GPR35 association with mitochondria. (A) Confocal microscopy of GPR35^{-/-} mouse neonatal cardiomyocytes stably expressing FLAG-tagged wild-type or R151A GPR35 that were treated with 20 μ M quinolinic acid, 20 μ M KynA, 1 μ M pamoic acid, or DMSO for 20 min. Scale bar, 20 μ m. (B) Immunoblot analysis of whole-cell extract (WCE) or mitochondria that were rapidly immunopurified by anti-HA immunoprecipitation (HA-IP) from 293T cells engineered to contain HA-tagged mitochondria (HA-MITO) or, as a control, FLAG-tagged mitochondria (FLAG-MITO). Where indicated, the cells were pretreated with 20 μ M KynA or 10 μ M zaprinast for 20 min before analysis. (C) GPR35^{-/-} mouse cardiomyocytes stably expressing FLAG-APEX-tagged wild-type or R151A GPR35 were treated with biotin-tryamide for 30 min and, where indicated, with 20 μ M KynA for 20 min and H_2O_2 for 1 min (to enable biotinylation). Cell lysates (WCE) and biotinylated proteins captured on streptavidin agarose (Strep-PD) were resolved by SDS-polyacrylamide gel electrophoresis (PAGE), transferred to nitrocellulose, and immunoblotted with antibodies against the indicated proteins or probed with horseradish peroxidase-conjugated streptavidin (Strep-HRP).

**Fig. 4. KynA promotes the GPR35-ATPIF1-ATP synthase interaction.**

(A) Immunoblot analysis of anti-FLAG immunoprecipitates (FLAG-IP) and WCE from mouse neonatal GPR35^{-/-} cardiomyocytes stably expressing GPR160-FLAG or GPR35-FLAG that were treated with 20 μM quinolinic acid, 20 μM KynA, 1 μM pamoic acid, 10 μM zaprinast, or DMSO for 20 min. (B) Immunoblot analysis of anti-FLAG immunoprecipitates from human AC16 cardiomyocytes stably expressing TMEM141-FLAG, GPR35 (wild-type)-FLAG, or GPR35 (ΔC terminus)-FLAG. (C) Immunoblot analysis of mitochondria isolated from mouse neonatal cardiomyocytes stably expressing GPR35-FLAG that were

treated with 20 μM KynA for 20 min. The isolated mitochondria were incubated with increasing concentrations of proteinase K (PK) for 30 min. (D) GPR35^{-/-} mouse neonatal cardiomyocytes stably expressing FLAG-APEX-tagged wild-type or R151A GPR35 were treated with biotin-tyramide for 30 min and, where indicated, with 20 μM KynA for 20 min and H₂O₂ for 1 min (to enable biotinylation). Cell lysates (WCE) and biotinylated proteins captured on streptavidin agarose (STREP-PD) were resolved by SDS-PAGE, transferred to nitrocellulose, and immunoblotted with the indicated proteins or probed with Strep-HRP.

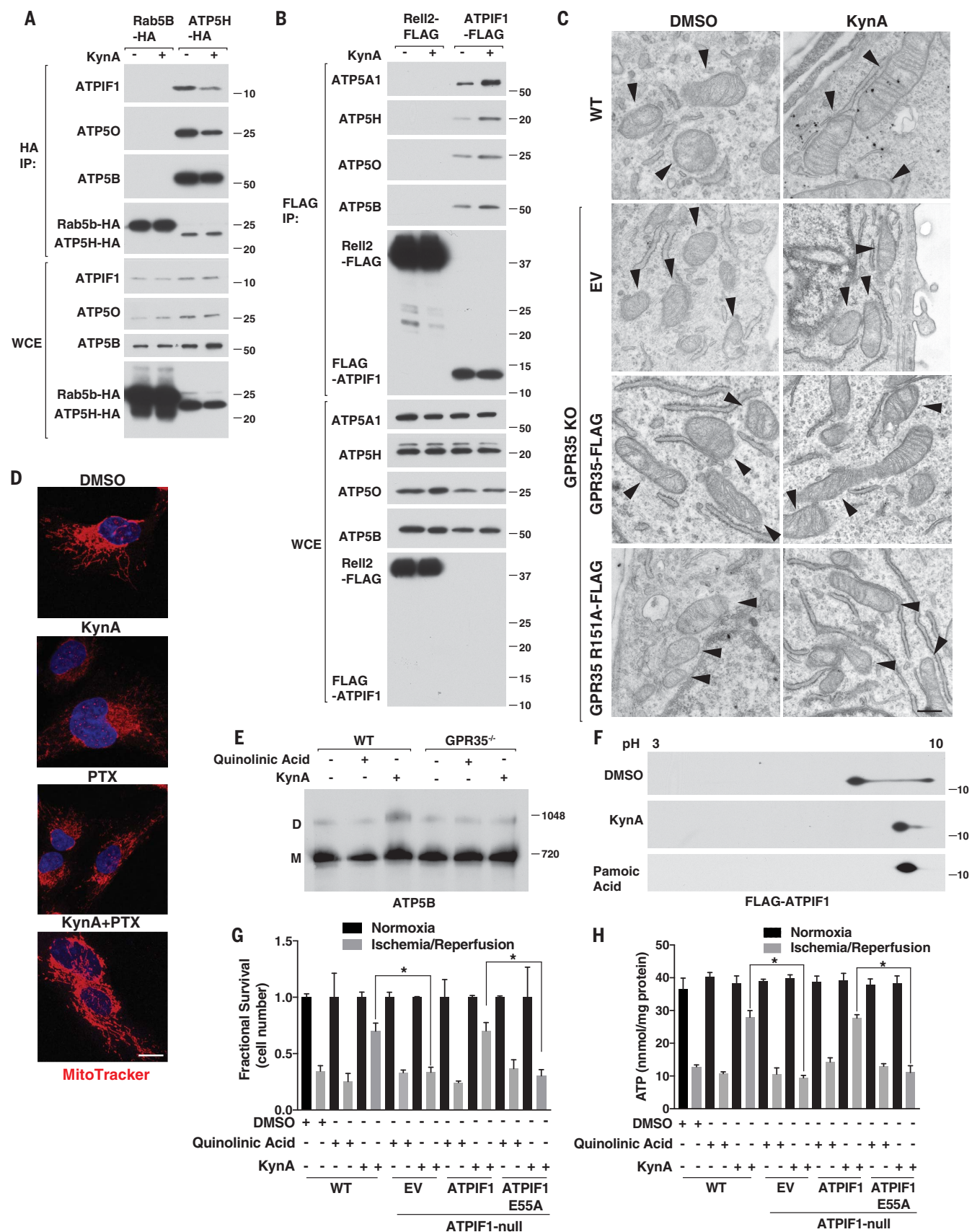


Fig. 5. KynA promotes ATP synthase dimerization and ATPIF1 is required for KynA-induced ischemic protection. (A) Immunoblot analysis of HA-IP and WCE from mouse neonatal cardiomyocytes stably expressing Rab5B-HA or ATP5H-HA that were or were not treated with 20 μM KynA for 20 min. (B) Immunoblot analysis of FLAG-IP and WCE from mouse neonatal cardiomyocytes stably expressing Rell2-FLAG or FLAG-ATPIF1 that were or were not treated with 20 μM KynA for 20 min. (C) Electron micrographs of wild-type and GPR35^{-/-} cardiomyocytes stably expressing GPR35-FLAG, R151A GPR35-FLAG, or empty vector (EV) that were treated with 20 μM KynA or DMSO for 20 min. Arrowheads indicate mitochondria. Scale bar, 500 nm. (D) Live-cell fluorescence imaging of mouse neonatal cardiomyocytes treated

with 20 μM KynA, 200 ng/ml PTX, or both before staining with 100 nM Mitotracker FM. Scale bar, 20 μm. (E) Blue-native page analysis of mitochondria isolated from mouse neonatal cardiomyocytes treated with 20 μM quinolinic acid, 20 μM KynA, or DMSO for 20 min. (F) Anti-Flag immunoblot analysis after two-dimensional gel electrophoresis of cell extracts made from mouse neonatal cardiomyocytes stably expressing FLAG-ATPIF1 that were treated with 20 μM KynA, 1 μM pamoic acid, or DMSO for 20 min. (G and H) Fractional survival (G) and ATP levels (H) of wild-type and ATPIF1^{-/-} hLPS-derived cardiomyocytes stably expressing wild-type or E55A ATPIF1 or EV that were pretreated with 20 μM KynA, 20 μM quinolinic acid, or DMSO for 1 hour before simulated I/R ex vivo. Data are shown as mean ± SD. *P < 0.05.

with the ATPIF1:ATP synthase stoichiometry shifting from 1:1 to 1:2 (Fig. 5, A and B, and fig. S11, A to D). We independently confirmed that KynA promotes ATP synthase dimerization using native gel electrophoresis and immunofluorescence and electron microscopy, which revealed hallmark changes in mitochondrial morphology and mitochondrial cristae, respectively, usually associated with ATP synthase dimerization (Fig. 5, C to E, and figs. S11E and S12, A to C) (46).

Because phosphorylation of ATPIF1 by PKA prevents it from inhibiting ATP synthase (47), we tested whether GPR35 activation caused dephosphorylation of ATPIF1. Both KynA and the GPR35 agonist pamoic acid blocked ATPIF1 phosphorylation in a GPR35-dependent manner, as shown by characteristic electrophoretic mobility changes after two-dimensional gel electrophoresis (Fig. 5F and fig. S12D).

We used CRISPR/Cas9 to generate ATPIF1^{-/-} cardiomyocytes from hLPS cells and then infected them with wild-type ATPIF1, an ATPIF1 point mutant that cannot bind to ATP synthase (ATPIF1 E55A), or an empty vector (fig. S13, A and B) (48). Wild-type ATPIF1, but not ATPIF1 E55A, allowed KynA to prevent ATP consumption and preserve cell viability during simulated ischemia ex vivo (Fig. 5, G and H). Collectively, these results show that KynA ischemic protection depends on ATPIF1.

Although GPCRs are typically thought to function at the plasma membrane, there are multiple examples of mitochondrial GPCRs and G proteins (49, 50). For example, the G protein guanine nucleotide binding protein-β subunit 2 (Gβ2) and guanine nucleotide binding protein subunit alpha-12 (Gα12) have roles in mitochondria fission versus fusion (51, 52). Moreover, many GPCRs, including GPR35, are internalized once activated, presumably so that they can signal in a spatially distinct manner (53). The endoplasmic reticulum has important roles in endosomal trafficking and forms multiple contacts with mitochondria, and a physical interaction between endosomes and mitochondria serves critical functions in cell homeostasis (54–56). The endosomal trafficking of GPR35 to mitochondria is reminiscent of Rab5, a small GTPase that translocates from early endosomes to mitochondria

in response to oxidative stress to confer cytoprotection (57).

We found that GPR35 could bind to ATPIF1 and that the latter is necessary for cardioprotection by former. Nonetheless, GPR35 associates with the mitochondrial outer membrane in response to KynA, whereas ATPIF1 is a mitochondrial matrix protein (47). Moreover, we did not detect biotinylation of ATPIF1 or ATP synthase by GPR35-APEX, and neither ATPIF1 nor ATP synthase was shown to be proteinase K sensitive. Thus, the interaction of GPR35 with ATPIF1 is not direct, but instead it is likely bridged by one or more proteins, perhaps at contact sites that have been demonstrated between outer and inner mitochondrial membranes and endosome-mitochondrial membrane contact sites (55, 58). Pertussis toxin did not block the internalization of GPR35 by KynA but blocked the KynA-mediated regulated interaction between ATPIF1 and ATP synthase, ATPIF1 dephosphorylation, and cardioprotection; the latter two therefore appear to be linked and to require G_{i/o} signaling (figs. S14A and S15A and Fig. 2D). We propose that GPR35, once activated and translocated to mitochondria, inhibits mitochondrial adenylate cyclase and thereby PKA. This, in turn, would allow ATPIF1 to promote ATP synthase dimerization and prevent ATP hydrolysis. Although KynA might have direct effects on mitochondria and may regulate metabolism, the effects that we observed clearly depend on GPR35 (59–65).

It is clear that ischemic preconditioning involves both an early and a late phase of ischemic protection, and we have shown that GPR35 is necessary for KynA-mediated cardioprotection whether administered acutely or 24 hours before I/R injury (Fig. 2A) (66). Although our data show that GPR35 is necessary in both settings, it remains unknown whether ATPIF1 is required at longer time scales.

Ischemic diseases such as myocardial infarction and stroke are major causes of death in the developed world. Remote ischemic preconditioning has been demonstrated in animal models, but attempts to harness it for therapeutic purposes in humans, such as through repeated hyperinflation of a limb blood pressure cuff before elective heart surgery, have not proven to be successful (67). Without an

understanding of the underlying mechanism, however, it was impossible to know whether the responsible tissue-protective factor was properly induced by these interventions and if its effects would be mitigated by other factors. Our findings support further exploration of KynA, and more broadly GPR35 agonists, for the prevention and treatment of ischemic injuries. A number of chemically synthetic GPR35 agonists have now been described, including compounds with far greater potency than KynA (20, 21). In addition, our findings provide a unifying explanation for the tissue-protective effects of kynurenine hydroxylase and kynurenine monooxygenase inhibitors. Although these inhibitors were originally developed to prevent the production of neuro-excitatory and neurotoxic tryptophan metabolites, they also promote the accumulation of KynA (68, 69).

REFERENCES AND NOTES

- B. A. Olenchock et al., *Cell* **164**, 884–895 (2016).
- C. E. Murry, R. B. Jennings, K. A. Reimer, *Circulation* **74**, 1124–1136 (1986).
- X. Zheng et al., *Exp. Mol. Med.* **51**, 1–14 (2019).
- L. Gelért et al., *Eur. J. Pharmacol.* **667**, 182–187 (2011).
- R. B. Nahomi et al., *Int. J. Mol. Sci.* **21**, 1795 (2020).
- N. Milani-Nejad, P. M. Janssen, *Pharmacol. Ther.* **141**, 235–249 (2014).
- C. Hilmas et al., *J. Neurosci.* **21**, 7463–7473 (2001).
- T. W. Stone, *Eur. J. Neurosci.* **25**, 2656–2665 (2007).
- M. H. Mok, A. C. Fricker, A. Weil, J. N. Kew, *Neuropharmacology* **57**, 242–249 (2009).
- F. Resta et al., *Neuropharmacology* **108**, 136–143 (2016).
- J. Wang et al., *J. Biol. Chem.* **281**, 22021–22028 (2006).
- B. C. DiNatale et al., *Toxicol. Sci.* **115**, 89–97 (2010).
- D. Wang et al., *Acta Pharm. Sin. B* **11**, 763–780 (2021).
- K. D. Min et al., *Biochem. Biophys. Res. Commun.* **393**, 55–60 (2010).
- V. P. Ronkainen et al., *Cardiovasc. Res.* **101**, 69–77 (2014).
- K. Chen et al., *J. Cardiovasc. Pharmacol.* **75**, 556–563 (2020).
- O. Sharmin et al., *Sci. Rep.* **10**, 9400 (2020).
- L. Olivares-González et al., *PLOS ONE* **11**, e0166717 (2016).
- G. Milligan, *Trends Pharmacol. Sci.* **32**, 317–325 (2011).
- Y. Taniguchi, H. Tonai-Kachi, K. Shinjo, *FEBS Lett.* **580**, 5003–5008 (2006).
- P. Zhao et al., *Mol. Pharmacol.* **78**, 560–568 (2010).
- A. E. MacKenzie et al., *Mol. Pharmacol.* **85**, 91–104 (2014).
- L. Jenkins et al., *Br. J. Pharmacol.* **162**, 733–748 (2011).
- P. Zhao et al., *J. Biol. Chem.* **289**, 3625–3638 (2014).
- E. V. Moo, J. R. van Senten, H. Bräuner-Osborne, T. C. Möller, *Mol. Pharmacol.* **99**, 242–255 (2021).
- H. Yang, H. Wang, R. Jaenisch, *Nat. Protoc.* **9**, 1956–1968 (2014).
- H. Deguchi et al., *Circ. J.* **84**, 1028–1033 (2020).
- W. Bao et al., *J. Cardiovasc. Pharmacol.* **56**, 147–155 (2010).
- T. L. Yeh et al., *Chem. Sci.* **8**, 7651–7668 (2017).
- J. I. Nwogu et al., *Circulation* **104**, 2216–2221 (2001).
- M. Vogler et al., *Pflügers Arch.* **467**, 2141–2149 (2015).
- M. Hölscher et al., *J. Biol. Chem.* **286**, 11185–11194 (2011).

33. J. D. Thornton, G. S. Liu, J. M. Downey, *J. Mol. Cell. Cardiol.* **25**, 311–320 (1993).
34. E. L. Huttlin et al., *Cell* **184**, 3022–3040.e28 (2021).
35. W. W. Chen, E. Freinkman, T. Wang, K. Birsoy, D. M. Sabatini, *Cell* **166**, 1324–1337.e11 (2016).
36. S. S. Lam et al., *Nat. Methods* **12**, 51–54 (2015).
37. S. Y. Lee et al., *Cell Rep.* **15**, 1837–1847 (2016).
38. C. Dong, C. M. Filipeanu, M. T. Duvernay, G. Wu, *Biochim. Biophys. Acta* **1768**, 853–870 (2007).
39. M. Fujikawa, H. Imamura, J. Nakamura, M. Yoshida, *J. Biol. Chem.* **287**, 18781–18787 (2012).
40. G. J. Grover et al., *Am. J. Physiol. Heart Circ. Physiol.* **287**, H1747–H1755 (2004).
41. J. J. García, E. Morales-Ríos, P. Cortés-Hernandez, J. S. Rodríguez-Zavala, *Biochemistry* **45**, 12695–12703 (2006).
42. L. Formentini, M. Sánchez-Aragó, L. Sánchez-Cenizo, J. M. Cuevva, *Mol. Cell* **45**, 731–742 (2012).
43. L. Sánchez-Cenizo et al., *J. Biol. Chem.* **285**, 25308–25313 (2010).
44. L. Formentini et al., *EMBO J.* **33**, 762–778 (2014).
45. F. Ibanez et al., *Br. J. Pharmacol.* **171**, 4193–4206 (2014).
46. A. García-Aguilar, J. M. Cuevva, *Front. Physiol.* **9**, 1322 (2018).
47. J. García-Bermúdez et al., *Cell Rep.* **12**, 2143–2155 (2015).
48. N. Ichikawa et al., *J. Biochem.* **130**, 687–693 (2001).
49. R. Valenzuela et al., *Cell Death Dis.* **7**, e2427 (2016).
50. A. Belous et al., *J. Cell. Biochem.* **92**, 1062–1073 (2004).
51. J. Zhang et al., *Nat. Commun.* **1**, 101 (2010).
52. A. V. Andreeva, M. A. Kutuzov, T. A. Voyno-Yasenetskaya, *FASEB J.* **22**, 2821–2831 (2008).
53. B. T. Lobingier, M. von Zastrow, *Traffic* **20**, 130–136 (2019).
54. A. D. Sheftel, A. S. Zhang, C. Brown, O. S. Shirihai, P. Ponka, *Blood* **110**, 125–132 (2007).
55. K. Todkar, L. Chikhi, M. Germain, *Mitochondrion* **49**, 284–288 (2019).
56. Y. Elbaz-Alon et al., *Nat. Commun.* **11**, 3645 (2020).
57. F. Hsu et al., *eLife* **7**, e32282 (2018).
58. A. S. Reichert, W. Neupert, *Biochim. Biophys. Acta* **1592**, 41–49 (2002).
59. H. Baran et al., *Int. J. Tryptophan Res.* **9**, 17–29 (2016).
60. H. Baran et al., *Pharmacology* **62**, 119–123 (2001).
61. H. Baran et al., *Life Sci.* **72**, 1103–1115 (2003).
62. D. Y. Lee et al., *Eur. J. Cell Biol.* **87**, 389–397 (2008).
63. L. Juhász et al., *Front. Med. (Lausanne)* **7**, 566582 (2020).
64. G. Schneditz et al., *Sci. Signal.* **12**, eaau9048 (2019).
65. L. Z. Agudelo et al., *Cell Metab.* **27**, 378–392.e5 (2018).
66. R. Bolli, *Circ. Res.* **87**, 972–983 (2000).
67. D. J. Hausenloy et al., *N. Engl. J. Med.* **373**, 1408–1417 (2015).
68. D. Zwilling et al., *Cell* **145**, 863–874 (2011).
69. A. Cozzi, R. Carpenedo, F. Moroni, J. Cereb. Blood Flow Metab. **19**, 771–777 (1999).

ACKNOWLEDGMENTS

We thank the members of the Kaelin laboratory and J. Moslehi (UCSF) for helpful discussions and critical reading of the manuscript. Special thanks go to the Cardiovascular Physiology Core (Longwood) at BWH/HMS for assistance with cardiac physiology experiments, as well as B. Olenchock and R. Liao for experimental advice. We also thank T. Sakmar for critical reading of the manuscript and V. Mootha for helpful discussions and experimental advice. **Funding:** W.G.K. is supported by the National Institutes of Health (grant 5R35CA210068) and is an Howard Hughes Medical Institute (HHMI) investigator. G.A.W. is an HHMI Fellow of the Jane Coffin Childs Memorial Fund for Medical Research. I.P.D. is a Fellow of the George and Marie Vergottis Foundation. J.D.M. is supported by Richard A. and Susan F. Smith President's Innovation Award, the Sidman Family Foundation, the Michael B. Rukin Charitable Foundation, the Kenneth C. Griffin Charitable Research Fund, The George and Marie Vergottis Foundation, and the Boston Investment Council. **Author contributions:** G.A.W. performed experiments and, together with W.G.K., designed experiments, analyzed data, and assembled and wrote the manuscript. W.Y. performed two-dimensional gel electrophoresis experiments and assisted in biochemical isolation of GPCRs. I.P.D., R.S.N., M.Y.S., and T.D. designed and performed the rabbit I/R model experiments under the direction and guidance of J.D.M. **Competing interests:** W.G.K. has financial interests in Lilly Pharmaceuticals, Fibrogen, Cedilla Therapeutics, IconOvir Bio, Nextech Invest, Tango Therapeutics, LifeMine Therapeutics, Circle Pharma, and Casdin Capital. J.D.M. is a consultant for Cellvive Scientific, Inc. The remaining authors declare no competing interests. **Data and materials availability:** All data needed to evaluate and reproduce the conclusions in the paper are present in the paper and/or the supplementary materials. All plasmids are available from the authors at request. **License information:** Copyright © 2022 the authors, some rights reserved; exclusive licensee American Association for the Advancement of Science. No claim to original US government works. <https://www.science.org/about/science-licenses-journal-article-reuse>

SUPPLEMENTARY MATERIALS

science.org/doi/10.1126/science.abm1638
Materials and Methods
Figs. S1 to S15
References (70–74)
MDAR Reproducibility Checklist

[View/request a protocol for this paper from Bio-protocol.](https://www.jove.com/video/50000)

Submitted 30 August 2021; accepted 28 June 2022
[10.1126/science.abm1638](https://science.org/doi/10.1126/science.abm1638)